Delft University of Technology

Delft Center for Systems and Control

Technical report 15-020

Model predictive control for freeway networks based on multi-class traffic flow and emission models*

S. Liu, H. Hellendoorn, and B. De Schutter

If you want to cite this report, please use the following reference instead:
S. Liu, H. Hellendoorn, and B. De Schutter, "Model predictive control for freeway networks based on multi-class traffic flow and emission models," *IEEE Transactions on Intelligent Transportation Systems*, vol. 18, no. 2, pp. 306–320, Feb. 2017.

Delft Center for Systems and Control
Delft University of Technology
Mekelweg 2, 2628 CD Delft
The Netherlands
phone: +31-15-278.51.19 (secretary)
fax: +31-15-278.66.79
URL: `http://www.dcsc.tudelft.nl`

*This report can also be downloaded via `http://pub.deschutter.info/abs/15_020.html`

Model Predictive Control for Freeway Networks Based on Multi-Class Traffic Flow and Emission Models

Shuai Liu, Hans Hellendoorn, and Bart De Schutter

***Abstract*—The main aim of this paper is to use multi-class macroscopic traffic flow *and* emission models for MPC for traffic networks. Particularly, we use and compare extended versions of multi-class METANET, FASTLANE, multi-class VT-macro, and multi-class VERSIT+. Besides, end-point penalties based on these multi-class traffic flow and emission models are also included in the objective function of MPC to account for the behavior of the traffic system beyond the prediction horizon. A simulation experiment is implemented to evaluate the multi-class models. The results show that the approaches based on multi-class METANET and the extended emission models (multi-class VT-macro or multi-class VERSIT+) can improve the control performance for the total time spent and the total emissions w.r.t. the non-control case, and they are more capable of dealing with the queue length constraints than the approaches based on FASTLANE. Including end-point penalties can further improve the control performance with a small sacrifice in the computational efficiency for the approaches based on multi-class METANET, but not for the approaches based on FASTLANE.**

I. Introduction

There are many ways to realize traffic management. Online model-based control is a popular approach in literature [1–4], and it can provide satisfying performance since it takes the predicted future evolution of traffic flows into account. In this kind of control approach, traffic models are necessary to describe the evolution of traffic states. Hence, appropriate traffic models are important for efficient online model-based traffic control. Many traffic models have been developed for describing traffic flows, emissions, and fuel consumption. In general, microscopic models are more accurate than macroscopic models because they describe the states of individual vehicles. However, this also implies that microscopic models are often time-consuming when simulating large-scale networks. In order to reduce the computation load, macroscopic traffic models are often used in online model-based traffic control. Many macroscopic models are homogeneous, and this means that the differences among different kinds of vehicles are neglected. Real traffic networks subsume various types of vehicles, such as cars, vans, trucks, etc. This leads to the need of macroscopic models that can describe the heterogeneous nature of real traffic networks.

Delft Center for Systems and Control, Delft University of Technology, Delft, The Netherlands. E-mail: {s.liu-1, j.hellendoorn, b.deschutter}@tudelft.nl.

Some first-order multi-class macroscopic traffic flow models have been developed by researchers. Wong and Wong [5] extended the Lighthill-Whitham-Richards (LWR) model [6, 7] to a multi-class version, in which the essential characteristics of each vehicle class remain unchanged, i.e. the states of each vehicle class depend on its own fundamental diagram and the total density. They validated that the multi-class LWR model can reproduce some traffic phenomena that the single-class LWR model cannot reproduce, e.g. two-capacity phenomena, hysteresis phenomena of phase transition, and platoon dispersion. Logghe [8] also developed a multi-class version of the LWR model, where each class is subject to its own fundamental diagram, and is considered to be limited within assigned space of the road. Van Lint et al. [9] proposed the FASTLANE model, which is a first-order multi-class macroscopic model. Here dynamic passenger car equivalents are used to describe different vehicle classes, taking into account the differences in the space occupied by a vehicle class under different traffic conditions (e.g. different densities). Schreiter et al. [10] proposed a multi-class controller based on FASTLANE, specifically rerouting the different traffic classes, and proved that a multi-class controller can improve the control performance more than a single-class controller. In the conference paper [11], Liu et al. extended FASTLANE with variable speed limits and ramp metering, and showed by a case study that MPC based on a multi-class prediction model can improve the performance more than MPC based on a single-class prediction model.

According to the literature [12–14], in general second-order models are more accurate than first-order models, due to the fact that second-order models can avoid certain non-realistic phenomena generated in first-order models. For instance, at the head and tail of shock waves (or traffic jams), the abrupt change in speed resulting from the large change in density in first-order models does not correspond to reality. Besides, in first-order models the tail of a shock wave has a higher speed than the high-density body of the shock wave, and the tail will catch up with the body, causing an unrealistically sharp rear end of the shock wave. In addition, first-order models cannot reproduce capacity drop near on-ramps and in shock waves, while second-order models can reproduce this capacity drop.

The METANET model is a second-order traffic flow model, which has also been extended to multi-class by some researchers. Deo et al. [15] proposed a multi-class version of the METANET model [16, 17] in which passenger car

equivalents are used to represent different vehicle classes. For the multi-class METANET model of Deo et al. [15], the total effective density, the joint maximum density, and the joint critical density are considered to be the same for all vehicle classes. Two options are considered by Deo et al. [15] for computing the desired speeds for different vehicle classes. One option is to use the convex combination of all class-dependent fundamental diagrams, limited by the desired speed of the given vehicle class; the other option is to use the same approach as in FASTLANE: when the total effective density is larger than the joint critical density, the fundamental diagram is the same for all vehicle classes; otherwise, the fundamental diagram differs for different vehicle classes due to class-dependent free-flow speeds. Deo et al. [15] showed by a numerical experiment that based on multi-class METANET the control performance can be improved more than that for single-class METANET. Pasquale et al. [18] extended the METANET model to a two-class version, where a convection factor between cars and trucks, which is analogous to passenger car equivalents, is used for describing different vehicle classes. Similarly to [15], the total density, the maximum density, and the critical density in terms of cars are considered to be the same for both cars and trucks. The difference with the multi-class METANET model in [15] lies in the way the fundamental diagram (i.e. the relation between desired speed and density) for a vehicle class is defined. In [18], the desired speed of a vehicle class depends on class-specific parameters and the total density. The difference in the critical densities for different vehicle classes is not considered in the above two versions of the multi-class METANET model.

The multi-class METANET model we use is based on the method that is used by Logghe [8] for developing the multi-class LWR model, where the difference in the critical densities for different vehicle classes is taken into account. It is assumed that each vehicle class is constrained within an assigned space of the road, being subject to its own fundamental diagram. Road space fractions are introduced for describing the assigned space for different vehicle classes. The actual density divided by the road space fraction for a vehicle class is considered to be the effective density for that vehicle class. Thus it is possible to describe the phenomenon that different classes transit to the congestion mode in different traffic conditions (i.e. at different densities). In particular, due to the difference in the critical densities for different vehicle classes, when a faster vehicle class is in the congestion mode (i.e. the effective density is larger than the critical density), a slower vehicle class may still be in the free-flow mode (i.e. the effective density is less than the critical density). In the conference paper [19], Liu et al. extended METANET to a multi-class version based on the above mentioned theory and validated through a numerical experiment that multi-class METANET can reduce the total time spent more than single-class METANET.

Traffic emission and fuel consumption models are necessary for the reduction of traffic emissions and fuel consumption in online model-based traffic control. Many microscopic emission and fuel consumption models have been developed for describing the emissions and fuel consumption of individual vehicles. These emission and fuel consumption models can be classified according to their inputs. Some emission and fuel consumption models use the vehicle speed as input, such as COPERT [20]. However, other emission and fuel consumption models use both the speed and the acceleration as inputs, e.g. VT-micro [21], VERSIT+ [22]. Macroscopic emission models can be used for reducing the computation load w.r.t. microscopic emission models. Csikos et al. [23] extended the COPERT model into a macroscopic version by introducing the concept of the spatiotemporal window. Pasquale et al. combined a multi-class version of METANET with COPERT in [18]. Zegeye et al. [3] developed the VT-macro model by integrating the VT-micro model with METANET. In the conference paper [24] Liu et al. applied the VT-macro model in a multi-class setting by combining the VT-macro model with a multi-class version of METANET of [15]. In [25] Pasquale and Liu et al. also combined the VERSIT+ model with a multi-class version of the METANET model in [18].

The main contribution of this paper is that we use multi-class macroscopic traffic flow *and* emission models for MPC for traffic networks. In particular, we use and compare extended versions of multi-class METANET, FASTLANE, multi-class VT-macro, and multi-class VERSIT+. Moreover, we include *end-point penalties* based on the extended multi-class traffic flow and emission models in the objective function of MPC, so that the performance beyond the prediction horizon can be captured. MPC is used as the control approach, considering that it can deal with nonlinear systems, multi-criteria optimization, and constraints. The Total Time Spent (TTS) and the Total Emissions (TE) are both included in the objective function of MPC for traffic networks, since we want to achieve a balanced trade-off between these two performance indicators.

This paper is organized as follows. In Section II, we introduce multi-class traffic flow models, including the FASTLANE model with extensions [11], and a multi-class METANET model previously extended by us [19]. In Section III, we introduce two emission models extended by the authors: multi-class VT-macro [24] and multi-class VERSIT+ [25]. In Section IV, we develop online MPC for freeway traffic networks. A simulation experiment is reported in Section V to compare the efficiency of these multi-class traffic models in online MPC for freeway networks.

II. Multi-Class Traffic Flow Models

In this paper, we develop online MPC for traffic networks. Considering the trade-off between computation complexity and accuracy, multi-class macroscopic traffic flow models will be adopted. In the remainder of this section, we represent the basic FASTLANE model [9], the extensions developed by the authors [11] for FASTLANE, and the multi-class METANET model extended by the authors in [19].

A. FASTLANE Model with Extensions

1) Basic FASTLANE Model: FASTLANE [9] is a first-order multi-class macroscopic traffic flow model that is represented by links (indexed by m), and each link is divided into several homogeneous cells (indexed by i). Here we give the discrete-time form of the FASTLANE model, since we use it within a MPC framework in this paper.

FASTLANE is a multi-class version of the LWR model. The main feature of FASTLANE is that it uses dynamic passenger car equivalents (pce) to transform different vehicle classes into a representative vehicle class. The different space occupied by vehicles under different traffic conditions (different traffic densities) is taken into account in the dynamic pce. In FASTLANE, the dynamic pce ($\theta_{m,i,c}$) for vehicle class c in cell i of link m is defined as

$$\theta_{m,i,c} = \frac{s_c + T_{h,c} \cdot v_{m,i,c}}{s_1 + T_{h,1} \cdot v_{m,i,1}} \tag{1}$$

in which $v_{m,i,c}$ is the speed of vehicle class c in cell i of link m, s_c is the gross stopping distance of vehicle class c, and $T_{h,c}$ is the minimum time headway of vehicle class c. The index 1 denotes the reference class.

Based on the dynamic pce, the effective density[1] ($\rho^{\text{efc}}_{m,i}$) in cell i of link m is defined as

$$\rho^{\text{efc}}_{m,i} = \sum_{c=1}^{n_c} \theta_{m,i,c} \rho_{m,i,c} \tag{2}$$

where $\rho_{m,i,c}$ is the density[1] of vehicle class c in cell i of link m, and n_c is the number of vehicle classes.

Since we use MPC in this paper, the discrete-time form of (2) is given as follows:

$$\rho^{\text{efc}}_{m,i}(k) = \sum_{c=1}^{n_c} \theta_{m,i,c}(k-1) \rho_{m,i,c}(k) \tag{3}$$

where k is the time step counter, which corresponds to the time instant $t = kT$, with T the simulation time interval.

Remark. *In order to ensure the stability of traffic flow models (e.g. FASTLANE and METANET), the Courant-Friedrichs-Lewy (CFL) [26] condition is often considered. In particular, no vehicle should cross a segment in one simulation time step T [13], i.e.*

$$T \leq \min_{m \in I_{\text{link}}} \frac{L_m}{v^{\text{free}}_{m,\max}} \tag{4}$$

where $v^{\text{free}}_{m,\max} = \max_{c=1,\ldots,n_c} v^{\text{free}}_{m,c}$ *is the free-flow speed of the fastest class of vehicles in link m,* $v^{\text{free}}_{m,c}$ *is the free-flow speed of vehicle class c in link m,* L_m *is the cell length of link m, and* I_{link} *is the set including all the links.*

For FASTLANE, the basic equations for computing flow, density, and speed of vehicle class c in cell i of link m are

$$q_{m,i,c}(k) = \mu_m \rho_{m,i,c}(k) v_{m,i,c}(k) \tag{5}$$

$$\rho_{m,i,c}(k+1) = \rho_{m,i,c}(k) + \frac{T}{L_m \mu_m} \left(q^{i-1,i}_{m,c}(k) - q^{i,i+1}_{m,c}(k) \right) \tag{6}$$

$$\begin{aligned} v_{m,i,c}(k) &= V_{m,c}(\rho^{\text{efc}}_{m,i}(k)) \\ &= \begin{cases} v^{\text{free}}_{m,c} - \rho^{\text{efc}}_{m,i}(k) \frac{(v^{\text{free}}_{m,c} - v^{\text{crit}}_m)}{\rho^{\text{crit}}_m} & \text{for } \rho^{\text{efc}}_{m,i}(k) < \rho^{\text{crit}}_m \\ \frac{v^{\text{crit}}_m \rho^{\text{crit}}_m}{\rho^{\text{efc}}_{m,i}(k)} \left(1 - \frac{\rho^{\text{efc}}_{m,i}(k) - \rho^{\text{crit}}_m}{\rho^{\text{max}}_m - \rho^{\text{crit}}_m} \right) & \text{for } \rho^{\text{efc}}_{m,i}(k) \geq \rho^{\text{crit}}_m \end{cases} \end{aligned} \tag{7}$$

with $q_{m,i,c}$ the flow of vehicle class c in cell i of link m, $q^{i,i+1}_{m,c}$ the flow of vehicle class c from cell i to cell $i+1$ of link m, v^{crit}_m the joint critical speed for all vehicle classes in link m, ρ^{crit}_m the joint critical density[1] for all vehicle classes in link m, ρ^{max}_m the effective maximum density[1] in link m, and μ_m the number of lanes of link m.

The traffic demand of cell i of link m needs to be distributed among different vehicle classes, according to the traffic composition in cell i of link m. This composition is represented by the flow ratio $\lambda_{m,i,c}$ of vehicle class c in cell i of link m:

$$\lambda_{m,i,c}(k) = \frac{\theta_{m,i,c}(k) q_{m,i,c}(k)}{\sum_{j=1}^{n_c} \theta_{m,i,j}(k) q_{m,i,j}(k)} \tag{8}$$

The flow of vehicle class c from cell i to cell $i+1$ of link m is described as follows:

$$q^{i,i+1}_{m,c}(k) = \frac{1}{\theta_{m,i,c}(k)} \min \left(D_{m,i,c}(k), \lambda_{m,i,c}(k) S_{m,i+1}(k) \right) \tag{9}$$

where the demand $D_{m,i,c}$ of vehicle class c and supply $S_{m,i}$ of all vehicle classes in cell i of link m are defined as

$$D_{m,i,c}(\rho^{\text{efc}}_{m,i}(k)) = \begin{cases} \mu_m \theta_{m,i,c}(k) \rho_{m,i,c}(k) V_{m,c}(\rho^{\text{efc}}_{m,i}(k)) & \\ \qquad \text{for } \rho^{\text{efc}}_{m,i}(k) < \rho^{\text{crit}}_m & \\ \mu_m \lambda_{m,i,c}(k) \rho^{\text{crit}}_m v^{\text{crit}}_m \quad \text{for } \rho^{\text{efc}}_{m,i}(k) \geqslant \rho^{\text{crit}}_m & \end{cases} \tag{10}$$

$$S_{m,i}(\rho^{\text{efc}}_{m,i}(k)) = \begin{cases} \mu_m \rho^{\text{crit}}_m v^{\text{crit}}_m & \text{for } \rho^{\text{efc}}_{m,i}(k) < \rho^{\text{crit}}_m \\ \mu_m \rho^{\text{efc}}_{m,i}(k) V_{m,c}(\rho^{\text{efc}}_{m,i}(k)) & \text{for } \rho^{\text{efc}}_{m,i}(k) \geqslant \rho^{\text{crit}}_m \end{cases} \tag{11}$$

For more details about FASTLANE, we refer to [9].

2) Extensions of FASTLANE: The FASTLANE model of [9] does not yield the queue lengths at origins (indexed by o). Besides, traffic control measures such as speed limits and ramp metering are also not included.

Just as in METANET [17], we introduce a simple queue equation for estimating the queue lengths at origins:

$$w_{o,c}(k+1) = w_{o,c}(k) + T(d_{o,c}(k) - q_{o,c}(k)) \tag{12}$$

where $w_{o,c}$ is the queue length of vehicle class c at origin o, $q_{o,c}$ is the flow of vehicle class c at origin o, and $d_{o,c}$ is the external demand of the vehicle class c at origin o.

Following the METANET speed equation of [27], a variable speed limit is incorporated in the speed equation as follows:

$$v_{m,i,c}(k) = \min(V_{m,c}(\rho^{\text{efc}}_{m,i}(k)), (1 + \delta_{m,c}) v^{\text{SL}}_{m,i}(k)) \tag{13}$$

where $v^{\text{SL}}_{m,i}$ is the speed limit that is applied in cell i of link m, and $1 + \delta_{m,c}$ is the non-compliance factor of vehicle class c in

[1]The effective density $\rho^{\text{efc}}_{m,i}$, the critical density ρ^{crit}_m, and the effective maximum density ρ^{max}_m are expressed in pce/km/lane, the density $\rho_{m,i,c}$ of vehicle class c in cell i of link m is expressed in vehicle/km/lane.

link m, which allows for modeling enforced and unenforced variable speed limits.

In order to apply ramp metering in traffic networks, the on-ramp flow equation with a ramp metering is defined as

$$q_{o,c}(k)=\frac{1}{\theta_{o,c}(k)}\min\left(r_o(k)D_{o,c}(k),\Lambda_o\lambda_{o,c}(k)S_{m,1}(k)\right) \tag{14}$$

in which $(m,1)$ indicates the cell to which the on-ramp connects, $\theta_{o,c}$ is the dynamic pce for vehicle class c at on-ramp o, $D_{o,c}$ is the total demand of vehicle class c at on-ramp o, and $\lambda_{o,c}$ is equal to the traffic composition at on-ramp o set by the user, representing the share for vehicle class c among the total demand at on-ramp o. In addition, Λ_o is defined as $\Lambda_o=\frac{C_o^{\text{efc}}}{C_{m-1}^{\text{efc}}+C_o^{\text{efc}}}$, with C_o^{efc} (expressed in pce/h) the effective capacity of on-ramp o, C_{m-1}^{efc} (expressed in pce/h) the effective capacity of the upstream link $m-1$ of the link m that connects to on-ramp o.

B. Multi-Class METANET Model

The METANET model [16, 17] is a second-order macroscopic model that describes traffic networks with uniform links corresponding to freeway stretches. Nodes are used to represent on-ramps, off-ramps, or other changes in geometry. Each link is divided into several homogeneous segments, which are similar with the concept of cells[2] in FASTLANE. Based on the method that is used by Logghe for developing the multi-class LWR model [8], we have proposed a multi-class METANET model in [19].

The multi-class LWR model of [8] is based on *user optimum* and *optimal road use*. The interaction between vehicle classes is described based on the user optimum, i.e. all vehicle classes try to maximize their speeds as much as possible, and faster vehicles cannot affect the speeds of slower vehicles due to the anisotropy of multi-class traffic. In [8], optimal road use means that a vehicle class never occupies more space than what is necessary for maintaining the speed of that vehicle class. For developing the multi-class METANET model, we also consider the same assumptions.

It is assumed that each vehicle class is constrained within an assigned space of the road, being subject to its own fundamental diagram:

$$q_{m,i,c}=\alpha_{m,i,c}Q_c\left(\frac{\rho_{m,i,c}}{\alpha_{m,i,c}}\right) \tag{15}$$

where $Q_c(\rho_{m,i,c})=\mu_m\rho_{m,i,c}v_{m,i,c}$ is the flow function of vehicle class c, and $\alpha_{m,i,c}$ is the road space fraction of vehicle class c in segment i of link m, which is defined as the ratio between the assigned space and the whole road space. The road space fractions for different classes of vehicles are always nonnegative, with the sum of all fractions equal to 1:

$$\alpha_{m,i,c}\geqslant 0 \tag{16}$$

$$\sum_{c=1}^{n_c}\alpha_{m,i,c}=1 \tag{17}$$

[2]Note that in the reminder of this paper, cells are considered to be equivalent to segments.

The actual density divided by the road space fraction for a vehicle class is considered to be the effective density of that vehicle class. Similarly, the actual flow divided by the road space fraction for a vehicle class is considered to be the effective flow of that vehicle class.

1) Traffic Flow Equations for Multi-Class METANET: Referring to single-class METANET [16, 17], the equation for computing the flow $q_{m,i,c}$ of vehicle class c in segment i of link m is the same as (5), and the equation for computing the queue length $w_{o,c}$ of vehicle class c at origin o is the same as (12). The density $\rho_{m,i,c}$ of vehicle class c in segment i of link m is computed as follows:

$$\rho_{m,i,c}(k+1)=\rho_{m,i,c}(k)+\frac{T}{L_m\mu_m}(q_{m,i-1,c}(k)-q_{m,i,c}(k)) \tag{18}$$

Class-dependent parameters ($\tau_{m,c}$, $\eta_{m,c}$, $\kappa_{m,c}$, $\rho_{m,c}^{\text{crit}}$, $v_{m,c}^{\text{free}}$, and $a_{m,c}$) are necessary for computing the speed $v_{m,i,c}$ and the origin flow $q_{o,c}$. The speed of vehicle class c in segment i of link m is described through the following equation:

$$\begin{aligned}v_{m,i,c}(k+1)=v_{m,i,c}(k)&+\frac{T}{\tau_{m,c}}\left(V_{m,c}\left(\frac{\rho_{m,i,c}(k)}{\alpha_{m,i,c}(k)}\right)-v_{m,i,c}(k)\right)\\&+\frac{T}{L_m}v_{m,i,c}(k)(v_{m,i-1,c}(k)-v_{m,i,c}(k))\\&-\frac{T\eta_{m,c}}{L_m\tau_{m,c}}\frac{\rho_{m,i+1,c}(k)-\rho_{m,i,c}(k)}{\rho_{m,i,c}(k)+\kappa_{m,c}}\end{aligned} \tag{19}$$

where $\tau_{m,c}$, $\eta_{m,c}$, and $\kappa_{m,c}$ are model parameters for vehicle class c in link m, and the desired speed function $V_{m,c}$ for vehicle class c in link m is defined as:

$$V_{m,c}\left(\frac{\rho_{m,i,c}(k)}{\alpha_{m,i,c}(k)}\right)=v_{m,c}^{\text{free}}\exp\left(\frac{-1}{a_{m,c}}\left(\frac{\rho_{m,i,c}(k)/\alpha_{m,i,c}(k)}{\rho_{m,c}^{\text{crit}}}\right)^{a_{m,c}}\right) \tag{20}$$

in which $a_{m,c}$ is a model parameter of vehicle class c in link m, and $\rho_{m,c}^{\text{crit}}$ is the critical density of vehicle class c in link m.

According to Hegyi et al. [27], a variable speed limit is included similarly to (13):

$$V_{m,c}\left(\frac{\rho_{m,i,c}(k)}{\alpha_{m,i,c}(k)}\right)=\min\left(V_{m,c}\left(\frac{\rho_{m,i,c}(k)}{\alpha_{m,i,c}(k)}\right),(1+\delta_{m,c})v_{m,i}^{\text{SL}}(k)\right) \tag{21}$$

The flow $q_{o,c}$ of vehicle class c at on-ramp o is

$$\begin{aligned}q_{o,c}(k)=\min\Bigg[&d_{o,c}(k)+\frac{w_{o,c}(k)}{T},r_o(k)\alpha_{m,1,c}(k)C_{o,c},\\&\alpha_{m,1,c}(k)C_{o,c}\left(\frac{\rho_{m,c}^{\max}-\rho_{m,1,c}(k)/\alpha_{m,1,c}(k)}{\rho_{m,c}^{\max}-\rho_{m,c}^{\text{crit}}}\right)\Bigg]\end{aligned} \tag{22}$$

with the index 1 representing the segment that the on-ramp is connected to in link m, $\alpha_{m,1,c}$ the road space fraction of vehicle class c in segment 1 of link m, $C_{o,c}$ the theoretical maximum capacity of on-ramp o if there would be only vehicle class c, $\rho_{m,c}^{\max}$ the theoretical maximum density of link m if there would be only vehicle class c, and $\rho_{m,1,c}$ the density of vehicle class c in segment 1 of link m.

For a mainstream origin o, the flow of vehicle class c is similar to the single-class equation developed in [27]:

$$q_{o,c}(k)=\min\left[d_{o,c}(k)+\frac{w_{o,c}(k)}{T},q_{m,1,c}^{\lim}(k)\right] \tag{23}$$

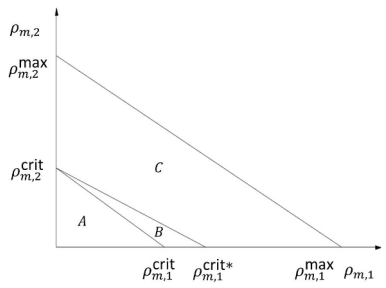

Fig. 1: Traffic regimes for two vehicle classes

where $q_{m,1,c}^{\lim}$ is the maximal inflow of vehicle class c for the first segment of link m that is connected to the origin:

$$q_{m,1,c}^{\lim}(k)=\begin{cases}\alpha_{m,i,c}(k)\mu_m\rho_{m,c}^{\text{crit}}v_{m,1,c}^{\lim}(k)\left[-a_{m,c}\ln\left(\frac{v_{m,1,c}^{\lim}(k)}{v_{m,c}^{\text{free}}}\right)\right]^{\frac{1}{a_{m,c}}} \\ \qquad\qquad \text{if } v_{m,1,c}^{\lim}(k)<V_{m,c}(\rho_{m,c}^{\text{crit}}) \\ \alpha_{m,i,c}(k)\mu_m\rho_{m,c}^{\text{crit}}V_{m,c}(\rho_{m,c}^{\text{crit}}) \quad \text{if } v_{m,1,c}^{\lim}(k)\geqslant V_{m,c}(\rho_{m,c}^{\text{crit}})\end{cases} \tag{24}$$

in which $v_{m,1,c}^{\lim}(k)=\min(v_{m,1}^{\text{SL}}(k),v_{m,1,c}(k))$ is the speed that limits the flow for vehicle class c in segment $(m,1)$, $v_{m,1}^{\text{SL}}$ is the speed limit of segment $(m,1)$, and $\alpha_{m,i,c}$ is used for converting effective flow to actual flow.

2) Road Space Fractions and Traffic Regimes: According to the densities for different vehicle classes, three traffic regimes are defined here, i.e. free-flow, semi-congestion, and congestion. The road space fractions are determined on the basis of these traffic regimes. Fig. 1 shows the traffic regimes for the case with two vehicle classes.

- Regime A: Free-Flow
  In the free-flow regime, the effective density of each vehicle class is less than or equal to its critical density. Therefore, the sufficient and necessary condition for the free-flow regime is

$$\frac{\rho_{m,i,c}(k)}{\alpha_{m,i,c}(k)}\leqslant\rho_{m,c}^{\text{crit}} \qquad \text{for all } c \tag{25}$$

  Based on (17) and (25), the constraint that separates the free-flow regime from the semi-congestion regime is obtained as follows:

$$\sum_{c=1}^{n_c}\frac{\rho_{m,i,c}(k)}{\rho_{m,c}^{\text{crit}}}\leqslant 1 \tag{26}$$

  According to (25), we define the space fraction of vehicle class c as

$$\alpha_{m,i,c}(k)=\frac{\rho_{m,i,c}(k)/\rho_{m,c}^{\text{crit}}}{\sum_{j=1}^{n_c}\rho_{m,i,j}(k)/\rho_{m,j}^{\text{crit}}} \tag{27}$$

- Regime B: Semi-Congestion
  From [8, 28], it could happen that slower vehicles are still in the free-flow regime, while faster vehicles are already in the congested mode. Thus in the multi-class setting, faster vehicle classes are considered to get in the congested mode earlier than slower vehicle classes, and the desired speeds of the congested vehicle classes are considered to be equal. The semi-congestion regime corresponds to the case that the desired speeds of the congested vehicle classes are larger than or equal to the desired speeds of slower vehicle classes that are still in the free-flow regime. In the semi-congestion regime, the effective density of at least one vehicle class is less than or equal to its critical density, and the effective density of at least one vehicle class is larger than its critical density.
  In order to obtain the boundary condition distinguishing the semi-congestion regime from the congestion regime, it is assumed that all vehicle classes are congested except for one vehicle class c_m^* that is on the verge of getting in the congested mode, i.e. the effective density of vehicle class c_m^* is equal to its critical density, resulting in the following road space fraction for vehicle class c_m^*:

$$\alpha_{m,i,c_m^*}(k)=\frac{\rho_{m,i,c_m^*}(k)}{\rho_{m,c_m^*}^{\text{crit}}} \tag{28}$$

  Actually, c_m^* is the vehicle class with the slowest desired speed when all vehicle classes are assumed to be on the verge of getting in the congested mode:

$$c_m^*=\underset{c=1,\ldots,n_c}{\arg\min}\left(v_{m,c}^{\text{free}}\exp\left(\frac{-1}{a_{m,c}}\right)\right) \tag{29}$$

  The following relation holds according to the definition of the semi-congestion regime:

$$V_{m,c_m^*}\left(\frac{\rho_{m,i,c_m^*}(k)}{\alpha_{m,i,c_m^*}(k)}\right)\leqslant V_{m,c}\left(\frac{\rho_{m,i,c}(k)}{\alpha_{m,i,c}(k)}\right) \quad \text{for} \quad c=1,\ldots,n_c \text{ with } c\neq c_m^* \tag{30}$$

  Considering (17), (28), and (30), the boundary condition distinguishing the semi-congestion regime from the congestion regime is obtained as follows:

$$\sum_{c=1}^{n_c}\frac{\rho_{m,i,c}(k)}{\rho_{m,c}^{\text{crit}*}}\leqslant 1 \tag{31}$$

  where $\rho_{m,c}^{\text{crit}*}$ is determined by the following equation:

$$\rho_{m,c}^{\text{crit}*}=\rho_{m,c}^{\text{crit}}\left[-a_{m,c}\ln\left(\frac{v_{m,c_m^*}^{\text{free}}}{v_{m,c}^{\text{free}}}\exp\left(\frac{-1}{a_{m,c_m^*}}\right)\right)\right]^{\frac{1}{a_{m,c}}} \tag{32}$$

  The proof of (31) and (32) is included in Appendix A.
  Suppose that $S_{m,i}^{\text{cong}}(k)$ denotes the set of all vehicle classes that are in congested mode in segment i of link m at time step k, and $S_{m,i}^{\text{free}}(k)$ denotes the set of all vehicle classes that are in free-flow mode in segment i of link m at time step k. The space fractions for the vehicle classes that are in free-flow mode are

$$\alpha_{m,i,c}(k)=\frac{\rho_{m,i,c}(k)}{\rho_{m,c}^{\text{crit}}} \qquad \text{for} \quad c\in S_{m,i}^{\text{free}}(k) \tag{33}$$

  The space fractions for the congested vehicle classes are obtained through solving the following system of

equations:

$$\begin{cases} V_{m,c}\left(\frac{\rho_{m,i,c}(k)}{\alpha_{m,i,c}(k)}\right) = V_{m,l_{m,i}}\left(\frac{\rho_{m,i,l_{m,i}}(k)}{\alpha_{m,i,l_{m,i}}(k)}\right) \\ \qquad\qquad \text{for} \quad c \in S_{m,i}^{\text{cong}}(k)/\{l_{m,i}\} \\ \sum_{c\in S_{m,i}^{\text{cong}}(k)} \alpha_{m,i,c}(k) = 1 - \sum_{\hat{c}\in S_{m,i}^{\text{free}}(k)} \alpha_{m,i,\hat{c}}(k) \end{cases} \tag{34}$$

where $l_{m,i}$ is an arbitrary element of the set $S_{m,i}^{\text{cong}}(k)$.

- Regime C: Congestion
  In the congestion regime, the effective density of each vehicle class is larger than its critical density; the desired speeds of all classes of vehicles are equal.
  The constraint for the congestion regime is the restriction on the maximum density:

$$\sum_{c=1}^{n_c} \frac{\rho_{m,i,c}(k)}{\rho_{m,c}^{\max}} \leqslant 1 \tag{35}$$

The space fractions can be derived by equating the desired speeds of all classes of vehicles:

$$\begin{cases} V_{m,1}\left(\frac{\rho_{m,i,1}(k)}{\alpha_{m,i,1}(k)}\right) = V_{m,2}\left(\frac{\rho_{m,i,2}(k)}{\alpha_{m,i,2}(k)}\right) \\ \qquad\vdots \\ V_{m,n_c-1}\left(\frac{\rho_{m,i,n_c-1}(k)}{\alpha_{m,i,n_c-1}(k)}\right) = V_{m,n_c}\left(\frac{\rho_{m,i,n_c}(k)}{\alpha_{m,i,n_c}(k)}\right) \\ \sum_{c=1}^{n_c} \alpha_{m,i,c}(k) = 1 \end{cases} \tag{36}$$

III. Multi-Class Traffic Emission Models

A. Multi-Class VT-Macro

The VT-macro model [3] is a macroscopic emission and fuel consumption model, which has been developed based on an integration of the VT-micro model [21] and the single-class METANET model [16, 17]. When the VT-macro model is used together with multi-class macroscopic traffic flow models, it is necessary to extend it to a multi-class setting too. In this section, we introduce the multi-class VT-macro model extended by the authors in [24], and this multi-class VT-macro model is an extension of the single-class VT-macro model in [3]. In the ensuing part of this section, the explanations are given for multi-class METANET and FASTLANE, but the multi-class VT-macro model can also be used for other multi-class macroscopic traffic flow models.

For each segment, two acceleration components are considered: inter-segment acceleration and cross-segment acceleration. For multi-class traffic flow, the accelerations for each class c are defined as follows:

$$a_{m,i,c}^{\text{inter}}(k) = \frac{v_{m,i,c}(k+1) - v_{m,i,c}(k)}{T} \tag{37}$$

$$a_{\alpha,\beta,c}^{\text{cross}}(k) = \frac{v_{\beta,c}(k+1) - v_{\alpha,c}(k)}{T} \tag{38}$$

where the indices α and β represent different adjacent segments, on-ramps, or off-ramps.

The numbers of vehicles corresponding to the above two components of accelerations are as follows:

$$n_{m,i,c}^{\text{inter}}(k) = L_m \mu_m \rho_{m,i,c}(k) - T q_{m,i,c}(k) \tag{39}$$

$$n_{\alpha,\beta,c}^{\text{cross}}(k) = T q_{\alpha,c}(k) \tag{40}$$

where $n_{m,i,c}^{\text{inter}}$ (expressed in veh) is the number of vehicles corresponding to $a_{m,i,c}^{\text{inter}}$, and $n_{\alpha,\beta,c}^{\text{cross}}$ (expressed in veh) is the number of vehicles corresponding to $a_{\alpha,\beta,c}^{\text{cross}}$.

The emission rates ($\text{EM}_{y,m,i,c}^{\text{inter}}$ and $\text{EM}_{y,\alpha,\beta,c}^{\text{cross}}$) for vehicle class c are as follows:

$$\text{EM}_{y,m,i,c}^{\text{inter}}(k) = n_{m,i,c}^{\text{inter}}(k) \exp\left(\tilde{v}_{m,i,c}^{T}(k) P_{y,c} \tilde{a}_{m,i,c}^{\text{inter}}(k)\right) \tag{41}$$

$$\text{EM}_{y,\alpha,\beta,c}^{\text{cross}}(k) = n_{\alpha,\beta,c}^{\text{cross}}(k) \exp\left(\tilde{v}_{\alpha,c}^{T}(k) P_{y,c} \tilde{a}_{\alpha,\beta,c}^{\text{cross}}(k)\right) \tag{42}$$

in which $P_{y,c}$ is a class-dependent parameter matrix, $y \in Y = \{\text{CO}, \text{NO}_x, \text{HC}, \text{fuel}\}$, and $\tilde{v}_{m,i,c}^{T}$, $\tilde{a}_{m,i,c}^{\text{inter}}$, $\tilde{v}_{\alpha,c}^{T}$, and $\tilde{a}_{\alpha,\beta,c}^{\text{cross}}$ are vectors in the form of $\tilde{x} = [1 \; x \; x^2 \; x^3]^T$.

The VT-macro model does not yield the emission rate of CO_2. According to [29], an approximate affine relationship exists between the emission rate for CO_2 and the fuel consumption rate. The emission rate $\text{EM}_{\text{CO}_2,m,i,c}$ for CO_2 for vehicle class c in segment i of link m can be estimated through

$$\text{EM}_{\text{CO}_2,m,i,c}(k) = \gamma_{1,c} v_{m,i,c}(k) + \gamma_{2,c} \text{EM}_{\text{fuel},m,i,c}(k) \tag{43}$$

where $\gamma_{1,c}$ and $\gamma_{2,c}$ are class-dependent model parameters, and $\text{EM}_{\text{fuel},m,i,c}$ is the fuel consumption rate for vehicle class c in segment i of link m given by

$$\text{EM}_{\text{fuel},m,i,c}(k) = \text{EM}_{\text{fuel},m,i,c}^{\text{inter}}(k) + \sum_{\alpha\in I_{m,i}^{\text{up}}} \text{EM}_{\text{fuel},\alpha,(m,i),c}^{\text{cross}}(k) \tag{44}$$

where $I_{m,i}^{\text{up}}$ is the set that includes all the upstream segments and origins that connect to segment (m,i).

Remark. *The approach for extending the multi-class VT-macro model is general in the sense that it can be used for any emission model using car characteristics, and with speeds and accelerations as inputs.*

B. Multi-Class VERSIT+

The VERSIT+ model [22] is a microscopic emission model developed based on a large number of emission tests. The VERSIT+ model requires a speed-data profile as input. Based on the VERSIT+ model in [22], we have extended a multi-class VERSIT+ model in [25] by the approach for extending the multi-class VT-macro model. In particular, the inter-segment acceleration and the cross-segment acceleration are also used here. The emission rate $\text{EM}_{y,m,i,c}^{\text{inter}}$ (expressed in g/s) based on the inter-segment acceleration of vehicle class c is

$$\text{EM}_{y,m,i,c}^{\text{inter}}(k) = \begin{cases} n_{m,i,c}^{\text{inter}}(k) u_{0,y,c} & \text{if } v_{m,i,c}(k) \leqslant 5,\ a_{m,i,c}^{\text{inter}}(k) \leqslant 0.5 \\ n_{m,i,c}^{\text{inter}}(k)\big(u_{1,y,c} + u_{2,y,c}(z_{m,i,c}^{\text{inter}}(k))_+ \\ \quad + u_{3,y,c}(z_{m,i,c}^{\text{inter}}(k) - 1)_+\big) & \text{if } 5 < v_{m,i,c}(k) \leqslant 50 \\ & \quad \text{or } v_{m,i,c}(k) \leqslant 5,\ a_{m,i,c}^{\text{inter}}(k) > 0.5 \\ n_{m,i,c}^{\text{inter}}(k)\big(u_{4,y,c} + u_{5,y,c}(z_{m,i,c}^{\text{inter}}(k))_+ \\ \quad + u_{6,y,c}(z_{m,i,c}^{\text{inter}}(k) - 1)_+\big) & \text{if } 50 < v_{m,i,c}(k) \leqslant 80 \\ n_{m,i,c}^{\text{inter}}(k)\big(u_{7,y,c} + u_{8,y,c}(z_{m,i,c}^{\text{inter}}(k) - 0.5)_+ \\ \quad + u_{9,y,c}(z_{m,i,c}^{\text{inter}}(k) - 1.5)_+\big) & \text{if } v_{m,i,c}(k) > 80 \end{cases} \tag{45}$$

where y represents emission categories (e.g. CO_2, NO_x, and PM10), $u_{0,y,c},\ldots,u_{9,y,c}$ are model parameters, and $z^{\text{inter}}_{m,i,c}$ is defined as

$$z^{\text{inter}}_{m,i,c}(k) = a^{\text{inter}}_{m,i,c}(k) + 0.014 v_{m,i,c}(k) \tag{46}$$

in which $a^{\text{inter}}_{m,i,c}$ (m/s^2) is the inter-segment acceleration of vehicle class c in segment i of link m, $v_{m,i,c}$ (km/h) is the speed of vehicle class c in segment i of link m, and $(x)_+ = \max(x,0)$.

The emission rate ($\text{EM}^{\text{cross}}_{y,\alpha,\beta,c}$) based on the cross-segment acceleration of vehicle class c is defined in a similar way as (45). In addition, the number of vehicles $n^{\text{inter}}_{m,i,c}$ and $n^{\text{cross}}_{\alpha,\beta,c}$ are computed through (39) and (40).

IV. Online Model Predictive Control for Traffic Network

A. Model Predictive Control

We choose Model Predictive Control (MPC) [30] for online traffic management, since it can deal with nonlinear systems, multi-criteria optimization, and constraints. MPC is a control approach based on dynamic prediction and a receding horizon scheme. In MPC, an objective function is used to capture the future performance of the system to be controlled over some prediction horizon. The controller determines the input sequence that optimizes the value of the objective function. According to the receding horizon scheme, only the first element of this optimal input sequence is applied to the controlled system.

In this paper, the main aim is to compare the extended multi-class traffic models (i.e. FASTLANE with extensions, multi-class METANET, multi-class VT-macro, and multi-class VERSIT+); thus, the extended models are used as prediction models of MPC for traffic networks. The control measures that we choose are variable speed limits and ramp metering. In addition, according to the literature [31, 32], in MPC for nonlinear systems the instability of the controlled system can be handled by including an end-point constraint or by using a large enough prediction horizon.

B. Performance Criteria

Various performance criteria can be considered when constructing the objective function for traffic management. In this paper, as an illustration, we consider the Total Time Spent (TTS) and the Total Emissions (TE).

The total time that all vehicles spend in the considered traffic network is denoted by Total Time Spent[3] (TTS), and defined as follows:

$$\text{TTS}(k_{\text{c}}) = T \sum_{j=k_{\text{c}}M}^{(k_{\text{c}}+N_{\text{p}})M-1} \sum_{c=1}^{n_{\text{c}}} p_c \left[\sum_{(m,i)\in I_{\text{all}}} \mu_m \rho_{m,i,c}(j) L_m + \sum_{o\in O_{\text{all}}} w_{o,c}(j) \right] \tag{47}$$

where I_{all} is the set of all pairs of link and segment indices (m,i) in the traffic network, O_{all} is the set of the indices of all origins, k_{c} is the control time step counter, which corresponds to the time instant $t = k_{\text{c}}T_{\text{c}}$ (with T_{c} the control time interval[4]), N_{p} is the prediction horizon, $M = T_{\text{c}}/T$ is assumed to be a positive integer, p_c indicates the passenger car equivalents (pce) for vehicle class c, and in this paper $p_c = s_c/s_1$.

The TE indicates the total emissions that all vehicles in the considered traffic network generate. The TE for emission type y is defined as

$$\text{TE}_y(k_{\text{c}}) = T \sum_{j=k_{\text{c}}M}^{(k_{\text{c}}+N_{\text{p}})M-1} \sum_{c=1}^{n_{\text{c}}} \left(\sum_{(m,i)\in I_{\text{all}}} \text{EM}^{\text{inter}}_{y,m,i,c}(j) + \sum_{\alpha,\beta\in P_{\text{all}}} \text{EM}^{\text{cross}}_{y,\alpha,\beta,c}(j) + \sum_{o\in O_{\text{all}}} \text{EM}^{\text{inter}}_{y,o,c}(j) \right) \tag{48}$$

in which P_{all} is the set of all pairs of adjacent segments and origins, and $\text{EM}^{\text{inter}}_{y,o,c}$ represents the emission rate of emission category y for vehicles in queue at origin o. The emission rate $\text{EM}^{\text{inter}}_{y,o,c}$ is computed in a similarly way as $\text{EM}^{\text{inter}}_{y,m,i,c}$, with vehicles in queue considered to have low speeds and no acceleration.

C. End-Point Penalties

In MPC for traffic networks, obtaining appropriate control performance may require a long prediction period, since it is recommended [27] to select the prediction period to be in the order of the typical travel time for a vehicle to cross the traffic network. This makes computation slow and complex for large-scale traffic networks. In this section, we present end-point penalties (which can be computed based on the multi-class traffic flow and emission models in Sections II-III) to take into account the performance of the considered traffic network beyond the prediction period.

1) End-Point Penalty Derived from the TTS: Based on the definition of the TTS, we present a TTS end-point penalty, which is an estimate of the TTS for all vehicles that are still in the network at time step $(k_{\text{c}}+N_{\text{p}})M$. Particularly, the TTS end-point penalty consists of the following parts:

- The number of vehicles in each segment multiplied by the time $t^{\text{rem}}_{m,i,c}((k_{\text{c}}+N_{\text{p}})M)$ that a vehicle that is present in that segment at time step $(k_{\text{c}}+N_{\text{p}})M$ would on the average need to get to its destination.
- The number of vehicles in each origin queue multiplied by the time $t^{\text{rem}}_{o,c}((k_{\text{c}}+N_{\text{p}})M)$ that a vehicle present in that origin queue at time step $(k_{\text{c}}+N_{\text{p}})M$ would on the average need to get to its destination.

The formula for computing the TTS end-point penalty is

$$\text{TTS}^{\text{end}}(k_{\text{c}}) = \sum_{c=1}^{n_{\text{c}}} \sum_{(m,i)\in I_{\text{all}}} \mu_m \rho_{m,i,c}((k_{\text{c}}+N_{\text{p}})M) L_m t^{\text{rem}}_{m,i,c}((k_{\text{c}}+N_{\text{p}})M) + \sum_{o\in O_{\text{all}}} w_{o,c}((k_{\text{c}}+N_{\text{p}})M) t^{\text{rem}}_{o,c}((k_{\text{c}}+N_{\text{p}})M) \tag{49}$$

[3]Note that the TTS index here includes the TTS for all segments, the TTS for all origins, and the TTS for all on-ramps, and they are treated equally, i.e. their weights are equal to 1.

[4]Note that in Sections II and III we assume $T_{\text{c}} = T$. Now we consider the general case with $T_{\text{c}} \neq T$.

2) End-Point Penalty Derived from the TE: Based on the definition of the TE, we present a TE end-point penalty, which is an estimate of the total emissions that the remaining vehicles at time step $(k_c+N_p)M$ generate before leaving the traffic network. The TE end-point penalty consists of the following two parts:

- The number of vehicles in each segment at time step $(k_c+N_p)M$ multiplied by the emissions $\mathrm{TE}^{\mathrm{rem}}_{y,m,i,c}((k_c+N_p)M)$ that a vehicle present in that segment at time step $(k_c+N_p)M$ would on the average generate before leaving the network.
- The number of vehicles in each origin queue at time step $(k_c+N_p)M$ multiplied by the emissions $\mathrm{TE}^{\mathrm{rem}}_{y,o,c}((k_c+N_p)$ that a vehicle present in that origin queue at time step $(k_c+N_p)M$ would on the average generate before leaving the network.

The formula for computing the TE end-point penalty is

$$\mathrm{TE}^{\mathrm{end}}_y(k_c)=\sum_{c=1}^{n_c}\sum_{(m,i)\in I_{\mathrm{all}}}\mu_m\rho_{m,i,c}((k_c+N_p)M)L_m\mathrm{TE}^{\mathrm{rem}}_{y,m,i,c}((k_c+N_p)M)+\sum_{o\in O_{\mathrm{all}}}w_{o,c}((k_c+N_p)M)\mathrm{TE}^{\mathrm{rem}}_{y,o,c}((k_c+N_p)M) \quad (50)$$

Remark. *Note that Origin-Destination (OD) matrices are needed for computing the end-point penalties, since they both depend on the destinations of vehicles. As reviewed in [33], OD matrices can be estimated based on traffic counts by means of both static methods [34] and dynamic methods [35]. In this paper, we just assume that a good estimate of the OD information is available.*

D. MPC Based on the Overall Objective Function

For different traffic conditions, the traffic control objectives may be conflicting [36]. We aim to achieve a balanced trade-off between the TTS and the TE here. However, the approach that we develop is generic, and it can also accommodate other performance indicators. Next, we will express the integrated control problem for reducing traffic congestion and traffic emissions in a systematic way. As examples, variable speed limits and ramp metering are chosen as control measures.

The overall objective function of the online traffic control in this paper is defined as follows:

$$\begin{aligned}J(k_c)=\;&\xi_{\mathrm{TTS}}\frac{\mathrm{TTS}(k_c)}{\mathrm{TTS}_{\mathrm{nom}}}+\sum_{y\in Y}\xi_{\mathrm{TE},y}\frac{\mathrm{TE}_y(k_c)}{\mathrm{TE}_{y,\mathrm{nom}}}\\&+\frac{\xi_{\mathrm{ramp}}}{N_cN_{\mathrm{RM}}}\sum_{l=k_c}^{k_c+N_c-1}\sum_{o\in O_{\mathrm{ramp}}}(r_o^{\mathrm{ctrl}}(l)-r_o^{\mathrm{ctrl}}(l-1))^2\\&+\frac{\xi_{\mathrm{speed}}}{N_cN_{\mathrm{VSL}}}\sum_{l=k_c}^{k_c+N_c-1}\sum_{(m,i)\in I_{\mathrm{speed}}}\left(\frac{v_{m,i}^{\mathrm{ctrl}}(l)-v_{m,i}^{\mathrm{ctrl}}(l-1)}{v_{m,\max}^{\mathrm{free}}}\right)^2\\&+\xi_{\mathrm{TTS}}^{\mathrm{end}}\frac{\mathrm{TTS}^{\mathrm{end}}(k_c)}{\mathrm{TTS}_{\mathrm{nom}}^{\mathrm{end}}}+\sum_{y\in Y}\xi_{\mathrm{TE},y}^{\mathrm{end}}\frac{\mathrm{TE}_y^{\mathrm{end}}(k_c)}{\mathrm{TE}_{y,\mathrm{nom}}^{\mathrm{end}}}\end{aligned} \quad (51)$$

where ξ_{TTS}, $\xi_{\mathrm{TE},y}$, ξ_{ramp}, ξ_{speed}, $\xi_{\mathrm{TTS}}^{\mathrm{end}}$, and $\xi_{\mathrm{TE},y}^{\mathrm{end}}$ are nonnegative weights, $\mathrm{TTS}_{\mathrm{nom}}$, $\mathrm{TE}_{y,\mathrm{nom}}$, $\mathrm{TTS}_{\mathrm{nom}}^{\mathrm{end}}$, and $\mathrm{TE}_{y,\mathrm{nom}}^{\mathrm{end}}$ are the corresponding "nominal" values for some nominal control profile (e.g. the no-control case), N_{RM} is the number of groups of metered on-ramps, and N_{VSL} is the number of groups of variable speed limits, O_{ramp} is the set of all metered on-ramps, I_{speed} is the set of all segments with speed limits, r_o^{ctrl} is the ramp metering rate of on-ramp o for a given control step, $v_{m,i}^{\mathrm{ctrl}}$ is the speed limit in segment i of link m for a given control step, and for $k=M(k_c-1)+1,\ldots,Mk_c$, $r_o(k)=r_o^{\mathrm{ctrl}}(k_c)$ and $v_{m,i}^{\mathrm{SL}}(k)=v_{m,i}^{\mathrm{ctrl}}(k_c)$. Note that the third and fourth terms of (51) are penalties to avoid abrupt variations in the control inputs.

The MPC problem based on the overall objective function is formulated as follows:

$$\min_{\substack{v_{m,i}^{\mathrm{ctrl}}(l),(m,i)\in I_{\mathrm{speed}}\\ r_o^{\mathrm{ctrl}}(l),o\in O_{\mathrm{ramp}}\\ l=k_c,\ldots,k_c+N_c-1}} J(k_c) \quad (52)$$

s.t. Traffic flow model equations

Traffic emission model equations

$$f(q_{m,i,c}(l),\rho_{m,i,c}(l),v_{m,i,c}(l),w_{o,c}(l))\leqslant 0 \quad \text{for } l=k_cM,\ldots,(k_c+N_p)M-1 \quad (53)$$

$$g(v_{m,i}^{\mathrm{ctrl}}(l),r_o^{\mathrm{ctrl}}(l))\leqslant 0 \quad \text{for } l=k_c,\ldots,k_c+N_c-1 \quad (54)$$

where the traffic flow model equations are those of the multi-class METANET model or the FASTLANE model, the traffic emission model equations are those of the multi-class VERSIT+ model or the multi-class VT-macro model, (53) represents a general constraint on traffic variables, and (54) represents a general constraint on variable speed limits and ramp metering rates. The above MPC problem is a general nonconvex problem, which can be solved using e.g. multi-start sequential quadratic programming, genetic algorithm, pattern search according to the literature [37, Chapter 5],[38, 39]

V. Benchmark Experiment

We now present a simulation experiment for comparing the multi-class traffic flow models and traffic emission models of Sections II-III, and for evaluating the effectiveness of the end-point penalties in Section IV-C.

A. Benchmark Network

The simulation experiment is based on the Dutch freeway A13, where we consider the direction from Rijswijk to Rotterdam, as shown in Fig. 2. The start of the considered part of the A13 is seen as the mainstream origin (O_0), and the end of the considered part of the A13 is seen as the mainstream destination (D_0). There are four on-ramps (O_1, O_2, O_3, and O_4) and four off-ramps (O_5, O_6, O_7, and O_8) each of which consists of a single lane, and all the on-ramps are metered. The main road subsumes three lanes, and variable speed limit signs are installed through the whole stretch in 15 positions in total. According to the location of on-ramps, off-ramps, and variable speed limit signs, the main road (7.8 km) is divided into 21 links, and in total 23 segments, i.e., most links only have 1 segment.

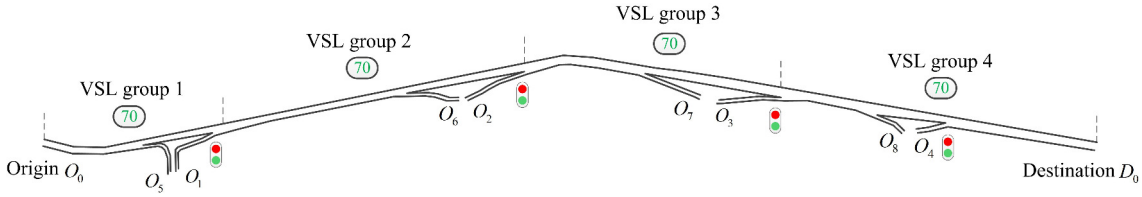

Fig. 2: Part of the Dutch freeway A13 considered in the case study

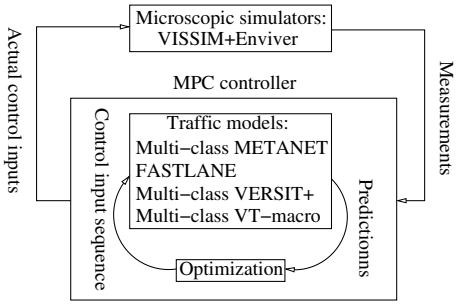

Fig. 3: Model predictive control for A13

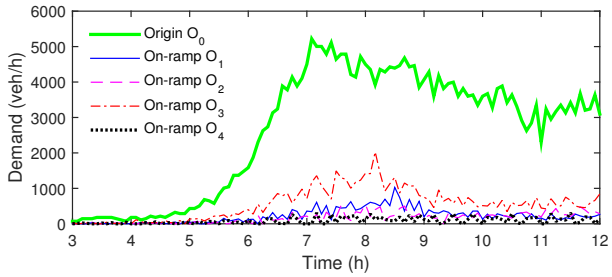

Fig. 4: Demands for A13

TABLE I: Validation errors for traffic flow models

	Scenario 1	Scenario 2	Scenario 3
Multi-class METANET	8.8%	9.2%	7.7%
FASTLANE	8.1%	7.4%	6.8%

TABLE II: Validation errors for emission models

	Scenario 1	Scenario 2	Scenario 3
Multi-class VERSIT+	2.6%	3.3%	4.3%
Multi-class VT-macro	1.1%	1.3%	1.4%

The microscopic simulators VISSIM and Enviver are used as process models for representing the real traffic network. VISSIM is used for simulating the traffic flows, and Enviver is used for simulating the emissions. The multi-class traffic flow and emission models in Sections II-III are used as prediction models in MPC. In both the process models and the prediction models, we consider two classes of vehicles (i.e. cars and trucks). The control procedure is shown in Fig. 3.

B. Identification of the Model Parameters

In order to describe the traffic flows and emissions by the models in Sections II and III, the parameters for these models need to be calibrated. The mainstream demand and the on-ramp demands for identification, which are shown in Fig. 4, are generated based on the field measurements of A13 on Feb. 18, 2014. The fraction of trucks in all the demands is taken as 0.1, considering the actual situation on the A13. These demands are used as the inputs for the microscopic simulator VISSIM. The model outputs are compared with the simulation outputs of VISSIM. Subsequently, the outputs from VISSIM are used as the inputs for Enviver. For multi-class METANET and FASTLANE, the objective for the identification procedure is to fit the TTS. Similarly, for multi-class VERSIT+ and multi-class VT-macro[5], the objective for the identification procedure is to fit the TE, where only CO_2 is considered. The optimizer "lsqnonlin" in MATLAB has been used for solving the calibration problem, based on the "trust-region-reflective" algorithm.

The prediction period length is chosen as 15 minutes, which corresponds to the average time needed for a vehicle to cross the freeway stretch under consideration. We consider the morning rush hours from 8.00 am to 10.00 am for the identification of the model parameters. For the period 8.00 am-10.00 am, the average calibration and validation errors within the prediction period between the measured TTS and the predicted TTS by METANET and FASTLANE are shown in Table I. The calibration and validation errors for multi-class VT-macro and multi-class VERSIT+ in the period 8.00 am-10.00 am are shown in Table II. Three scenarios for the traffic demands are considered for assessment:

- Scenario 1: the scenario used for identification;
- Scenario 2: Scenario 1 + sinusoidal noise (with an amplitude equal to 5% of the demands for Scenario 1, and with a cycle time of 15 minutes);
- Scenario 3: Scenario 1 + white noise (with an amplitude equal to 5% of the demands for Scenario 1).

According to Table I, both the calibration errors and the validation errors are comparable for multi-class METANET and FASTLANE. According to Table II, the calibration errors and the validation errors are also comparable for multi-class VERSIT+ and multi-class VT-macro.

Based on the model parameters obtained, the total fundamental diagram (basic flow-density relationship) of the extended multi-class METANET model is shown in Fig. 5.

C. Control Settings

Scenario 1 as shown in Fig. 4 is considered for control in this case study. The control time interval (T_c) is chosen

[5]Note that the effect that some cars may be stuck behind trucks can be indirectly included in these emission and fuel consumption models via the calibration of the model parameters.

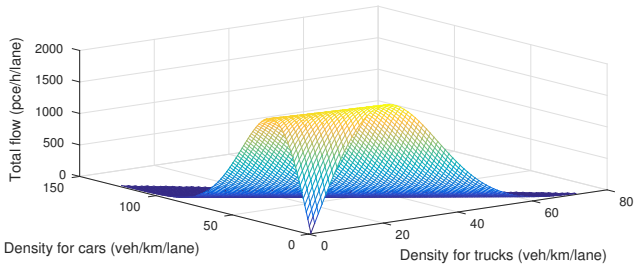

Fig. 5: Total fundamental diagram of multi-class METANET for cars and trucks

as 5 minutes, the control horizon is chosen as 10 minutes ($N_c = 2$), and the prediction horizon is chosen as 15 minutes ($N_p = 3$). The simulation time step (T) is selected to be 6 seconds, according to (4).

Recall that suppose that all four on-ramps are metered ($N_{RM} = 4$). According to the actual length of the on-ramps, the maximum permitted queue lengths (w_o^{max}, $o \in O_{ramp} = \{O_1, O_2, O_3, O_4\}$) are repetitively 100, 100, 200, 50 pce. There are 15 positions equipped with Variable Speed Limit (VSL), and we divide them into 4 groups ($N_{VSL} = 4$):

- VSL group 1: VSLs 1-4, i.e. VSLs before O_1;
- VSL group 2: VSLs 5-7, i.e. VSLs between O_1 and O_2;
- VSL group 3: VSLs 8-10, i.e. VSLs between O_2 and O_3;
- VSL group 4: VSLs 11-15, i.e. VSLs after O_3.

Considering that all segments are relatively short, we assume that vehicles in a segment without a variable speed limit sign are subject to the variable speed limit for the closest upstream segment with a variable speed limit sign.

As will be explained below, two groups of approaches are implemented for comparing multi-class macroscopic traffic flow models and traffic emission models in Sections II-III, and for investigating the effectiveness of the end-point penalties in Section IV-C.

1) Comparison for multi-class models: For the multi-class models, we compare four approaches *without* end-point penalties as follows:

- Approach A: Multi-class METANET and multi-class VERSIT+;
- Approach B: Multi-class METANET and multi-class VT-macro;
- Approach C: FASTLANE and multi-class VERSIT+;
- Approach D: FASTLANE and multi-class VT-macro.

For each approach, we consider 3 combinations of weights *without* end-point penalties (ξ_{TTS}^{end}=0, and ξ_{TE,CO_2}^{end}=0):

- Combination 1: ξ_{TTS}=1, ξ_{TE,CO_2}=0.1;
- Combination 2: ξ_{TTS}=0.5, ξ_{TE,CO_2}=0.5;
- Combination 3: ξ_{TTS}=0.1, ξ_{TE,CO_2}=1.

2) Comparison for end-point penalties: In order to show the effects of end-point penalties, we also implement the following four approaches:

- Approach E: multi-class METANET and multi-class VERSIT+ with end-point penalties;
- Approach F: multi-class METANET and multi-class VT-macro with end-point penalties;
- Approach G: FASTLANE and multi-class VERSIT+ with end-point penalties;
- Approach H: FASTLANE and multi-class VT-macro with end-point penalties.

As an illustration, we choose ξ_{TTS}=1 and ξ_{TE,CO_2}=0.1 (the same as in Combination 1) for Approaches E to H. For ξ_{TTS}=1 and ξ_{TE,CO_2}=0.1, an investigation has been done to find appropriate ξ_{TTS}^{end} and ξ_{TE,CO_2}^{end} for the end-point penalties; the values obtained are ξ_{TTS}^{end}=0.1 and ξ_{TE,CO_2}^{end}=0.01.

We solve the control problem with sequential quadratic programming based on a multi-start scheme. An investigation has been done in order to make the CPU time for the approaches including multi-class METANET and the approaches including FASTLANE roughly the same. Thus for Approaches A, B, E, and F, 50 starting points are used for every control step, and for C, D, G, and H, 70 starting points are used for every control step.

D. Results and Analysis

All simulations are implemented on a computer with 2 Intel(R) Xeon(R) CPU E5-1620 v3 @3.50GHz processors. For each approach and each combination of weights, 10 runs with different random seeds corresponding to different starting points for "fmincon" in MATLAB are implemented, and the average results are listed in Tables III-VI. In addition, we have also recorded the CPU time for each approach and each combination of weights, and the results are listed in Tables III-VI.

In these tables, $J_{TTS,TE}^{imp}$ represents the relative improvement of $J_{TTS,TE}$ over the entire simulation period w.r.t. the case without control, with $J_{TTS,TE}$ defined as

$$J_{TTS,TE} = \xi_{TTS} \frac{TTS_{tot}}{TTS_{nom}} + \xi_{TE,CO_2} \frac{TE_{CO_2,tot}}{TE_{CO_2,nom}} \tag{55}$$

where TTS_{nom} is the TTS over the prediction period for the no-control case computed at the first control step, TTS_{tot} is the total time spent over the entire simulation period, $TE_{CO_2,nom}$ is the TE of CO_2 over the prediction period for the no-control case computed at the first control step, and $TE_{CO_2,tot}$ represents the TE of CO_2 over the entire simulation period.

We define a total objective function J_{total} as follows:

$$J_{total} = J_{TTS,TE} + \xi_{queue} \max_{o \in O_{ramp}} \max \left(\max_{k=1,\ldots,k_{end}} \frac{\sum_{c=1}^{n_c} (p_c w_{o,c}(k))}{w_o^{max}} - 1, 0 \right) \tag{56}$$

where k_{end} is the last simulation time step of the entire simulation period, and w_o^{max} is the maximum permitted queue length for on-ramp o expressed in pce. The last term of J_{total} represents the maximum queue length constraint violation for all on-ramps over the entire simulation period, and the weight for this term is set to be a large value aiming at evaluating the satisfaction of queue length constraints: $\xi_{queue} = 10$. This total objective function is used for comparing the total performance including the TTS, the TE, and the queue length constraint violations, where higher values indicate a worse total performance.

TABLE III: Simulation results for Combination 1

Approaches	$J_{\text{TTS,TE}}^{\text{imp}}$	Constraint violations				J_{total}	CPU (h)
		O_1	O_2	O_3	O_4		
A	2.2%	0%	0%	0%	0%	8.6	7.7
B	2.4%	0%	0%	0%	0%	8.6	11.4
C	-5.7%	43.5%	0%	125.4%	0%	21.8	10.0
D	-8.6%	48.1%	14.6%	210.2%	0%	30.6	10.7

TABLE IV: Simulation results for Combination 2

Approaches	$J_{\text{TTS,TE}}^{\text{imp}}$	Constraint violations				J_{total}	CPU (h)
		O_1	O_2	O_3	O_4		
A	3.9%	0%	0%	0%	0%	7.7	7.0
B	2.4%	6.6%	0%	0%	0%	8.4	10.1
C	0.6%	10.2%	8.1%	229.2%	0%	30.8	10.7
D	0.2%	57.4%	0%	220.9%	0%	30.0	13.3

TABLE V: Simulation results for Combination 3

Approaches	$J_{\text{TTS,TE}}^{\text{imp}}$	Constraint violations				J_{total}	CPU (h)
		O_1	O_2	O_3	O_4		
A	6.8%	5.1%	0%	0%	0%	8.6	6.1
B	3.7%	26.5%	0%	0%	0%	11.0	8.9
C	13.1%	37.9%	23.8%	177.0%	0%	25.3	10.3
D	12.7%	107.1%	18.9%	188.7%	0%	26.5	12.9

TABLE VI: Simulation results for Combination 1 with end-point penalties

Approaches	$J_{\text{TTS,TE}}^{\text{imp}}$	Constraint violations				J_{total}	CPU (h)
		O_1	O_2	O_3	O_4		
E	3.5%	0%	0%	0%	0%	8.5	8.2
F	4.2%	0%	0%	0%	0%	8.4	12.4
G	-9.7%	57.2%	6.3%	236.3%	0%	33.3	8.0
H	-5.9%	69.0%	7.7%	157.8%	0%	25.1	10.0

In following two subsections we first compare Approaches A-D, then the effects of each extended multi-class traffic model can be analyzed. Next, we compare Approaches E-H with Approaches A-D, then the effects of end-point penalties can be analyzed.

1) Results for multi-class models without end-point penalties: The results for multi-class models *without* end-point penalties are listed in Tables III-V. According to Tables III-V, Approach A (multi-class METANET and multi-class VERSIT+) can improve the performance for TTS and TE ($2.2\% - 6.8\%$) w.r.t. the non-control case, with relatively small queue length constraint violations ($0\% - 5.1\%$); the queue length constraint violations only occur for Combination 3, which has a high weight for TE. Approach B (multi-class METANET and multi-class VT-macro) can also improve the performance for TTS and TE ($2.4\% - 3.7\%$) w.r.t. the non-control case, but the queue length constraint violations increase from 0% to 26.5% with the increase of the weight for TE. For Approach A, the values of J_{total} are less than those for Approach B for all the combinations of weights, i.e. the total performance for Approach A is better than the total performance for Approach B.

The approaches based on FASTLANE (C and D) lead to a worse performance for TTS and TE ($-8.6\% - -5.7\%$) than the no-control case for Combination 1, but a better performance for TTS and TE ($0.2\% - 13.1\%$) than the no-control case for Combination 2 and Combination 3. Note, however, that for all the combinations there are consistent queue length constraint violations for on-ramps O_1 ($10.2\% - 107.1\%$) and O_3 ($125.4\% - 229.2\%$). Thus the values of J_{total} ($21.8 - 30.8$) for the approaches based on FASTLANE (C and D) are much higher than the values ($7.7 - 11.0$) for the approaches based on multi-class METANET (A and B), i.e. the total performance for the former approaches is worse than that of the latter approaches.

High constraint violations can lead to traffic jams upstream of the given on-ramps, which is an important issue to be handled when a control approach is developed. For the settings of our experiment, the approaches based on multi-class METANET are more capable of dealing with the queue length constraints.

Comparing the CPU time for Approach A (which is based on multi-class METANET and multi-class VERSIT+) with that for Approach B (which is based on multi-class METANET and multi-class VT-macro), we find that Approach A is faster than Approach B for the 3 considered combinations of weights. Comparing the CPU time for Approach C (which is based on FASTLANE and multi-class VERSIT+) with that for Approach D (which is based on FASTLANE and multi-class VT-macro), we find that Approach C is faster than Approach D for the 3 considered combinations of weights.

2) Results for end-point penalties: The results for approaches with end-point penalties are included in Table VI, and these results are now compared with results in Table III. In comparison with the approaches based on multi-class METANET without end-point penalties (A and B in Combination 1), including end-point penalties (E and F) can further improve the performance for TTS and TE (3.5%-4.2%), while there is still no queue length constraint violation. In addition, the values of J_{total} (8.4-8.5) are also further reduced w.r.t. the approaches without end-point penalties. Thus, for approaches based on multi-class METANET we can say that end-point penalties can improve both the performance for TTS and TE and the total performance.

The approaches based on FASTLANE with end-point penalties (G and H) cannot reduce the high constraint violations for on-ramps O_1 (57.2%-69.0%) and O_3 (157.8%-236.3%) to a low level, and the values of J_{total} (25.1-33.3) are still much higher than those for the approaches based on multi-class METANET (A, B, E, and F). This might be because of the first-order characteristics of FASTLANE, which makes the estimations of end-point penalties less reliable.

Comparing the CPU time for Approaches A and B (which are based on multi-class METANET without end-point penalties) with that for Approaches E and F (which are based on multi-class METANET with end-point penalties), we find that when the end-point penalties are included the CPU time is increased by 6.5% for Approach A, and by 8.8% for Approach B. However, for the approaches based on FASTLANE, the CPU time for Approach G (with end-point penalties) is reduced compared to Approach C (without end-point penalties), and the CPU time for Approach H (with end-point penalties) is also reduced compared to

Approach D (without end-point penalties).

VI. Conclusions and Future Work

In this paper, we have compared extended multi-class traffic flow models (multi-class METANET and FASTLANE with extensions) and traffic emission models (multi-class VT-macro and multi-class VERSIT+). End-point penalties that are computed based on the extended multi-class traffic flow and emission models are included to account for the future evolution of the traffic system beyond the prediction period. Since the main aim is to compare the extended models, we have used them as prediction models for MPC for traffic networks based on the same setting. We have expressed the integrated control problem for reducing traffic congestion and traffic emissions in a systematic way, and the work in this paper can be seen as a proof of the concept for the integrated control approach for reducing traffic congestion and traffic emissions.

A simulation experiment has been implemented to compare these multi-class traffic flow models and traffic emission models, and to evaluate the effectiveness of the end-point penalties. Eight approaches have been considered for MPC for part of the Dutch freeway network A13, i.e., the four approaches based on the multi-class traffic flow models and traffic emission models, as well as these approaches with the end-point penalties. The results show that the approaches based on multi-class METANET can improve the performance for TTS and TE w.r.t. the no-control case with smaller queue length constraint violations than those for FASTLANE. The queue length constraint violations for multi-class METANET increase with the weight for TE, probably due to the fact that vehicles in queues are considered to generate less emissions than vehicles that are driving, since the vehicles in the queues have low speeds and almost no acceleration. For these approaches based on multi-class METANET, including end-point penalties can further improve the performance for TTS and TE and the total performance with a small sacrifice in the computational efficiency. On the other hand, for the given case study, the approaches based on FASTLANE lead to consistent queue length constraint violations, which may cause traffic jams upstream of the corresponding on-ramps; furthermore, for these approaches including end-point penalties cannot improve the total performance, probably due to the less reliable estimations of end-point penalties based on FASTLANE.

For future research, the VISSIM model parameters can be calibrated with real-world data. Extra identification for more scenarios, identification with flow and density calibrated, and identification through other algorithms could be done for model parameters. Besides, larger complex networks and more traffic scenarios can be investigated for validating the effectiveness of the extended multi-class traffic flow and emission models. Additionally, the impact of end-point penalties can also be further investigated by testing suitable weights for these penalties in different control conditions. Moreover, the comparison of the single-class METANET model and the multi-class METANET model can be implemented for multiple layouts and a wide range of scenarios based on microscopic simulators. When the size of the network increases, distributed model predictive control approach and parameterized control approach can be considered for reducing the computation time.

Acknowledgments

Research supported by the China Scholarship Council. We thank Goof van de Weg (Civil Engineering and Geosciences, Delft University of Technology) for providing the VISSIM model of the A13 freeway stretch that is used in the case study of this research.

Appendix A
Proof of the Boundary Condition for the Semi-Congestion Regime

Proof. The proof is based on (17), (20), (30), and (28). Substitute (20) into (30), and consider (28):

$$v_{m,c_m^*}^{\text{free}} \exp\left(\frac{-1}{a_{m,c_m^*}}\right) \leqslant v_{m,c}^{\text{free}} \exp\left(\frac{-1}{a_{m,c}} \left(\frac{\rho_{m,i,c}(k)}{\alpha_{m,i,c}(k)\rho_{m,c}^{\text{crit}}}\right)^{a_{m,c}}\right) \quad \text{for } c = 1,\ldots,n_{\text{c}} \text{ with } c \neq c_m^* \tag{57}$$

From (57), the following equation can be obtained:

$$\frac{\rho_{m,i,c}(k)}{\alpha_{m,i,c}(k)} \leqslant \rho_{m,c}^{\text{crit}} \left[-a_{m,c} \ln\left(\frac{v_{m,c_m^*}^{\text{free}}}{v_{m,c}^{\text{free}}} \exp\left(\frac{-1}{a_{m,c_m^*}}\right)\right)\right]^{\frac{1}{a_{m,c}}} \quad \text{for} \quad c = 1,\ldots,n_{\text{c}} \text{ with } c \neq c_m^* \tag{58}$$

The right-hand side of (58) is equal to $\rho_{m,c}^{\text{crit}*}$, cf. (32). Hence,

$$\frac{\rho_{m,i,c}(k)}{\rho_{m,c}^{\text{crit}*}} \leqslant \alpha_{m,i,c}(k) \quad \text{for} \quad c = 1,\ldots,n_{\text{c}} \text{ with } c \neq c_m^* \tag{59}$$

For vehicle class c_m^*, $\rho_{m,c_m^*}^{\text{crit}} = \rho_{m,c}^{\text{crit}*}$. Considering (17), the boundary condition for the semi-congestion regime can be obtained: $\sum_{c=1}^{n_{\text{c}}} \frac{\rho_{m,i,c}(k)}{\rho_{m,c}^{\text{crit}*}} \leqslant 1$, i.e. (31) in Section II-B.

Appendix B
Table of Notations

m	index for link;
i	index for segment (cell);
o	index for origin;
c	index for vehicle class;
c_m^*	vehicle class with the slowest desired speed in free-flow regime;
y	index for emission (fuel) category;
t	time instant;
k	simulation time step counter;
k_{c}	control time step counter;
k_{end}	last simulation time step of the entire simulation period;
T	simulation time step length;
T_{c}	control time step length;
M	positive integer defined by $M = T_{\text{c}}/T$;

N_{p} prediction horizon length;
N_{c} control horizon length;
n_{c} total number of vehicle classes;
L_m segment (cell) length of link m;
μ_m number of lanes of link m;
$q_{m,i,c}$ flow of vehicle class c in segment (cell) (m,i);
$q_{\alpha,c}$ flow of vehicle class c in segment (cell) α;
$q^{\mathrm{lim}}_{m,1,c}$ maximal inflow of vehicle class c for the first segment of link m that is connected to the origin;
$q_{o,c}$ flow of vehicle class c at origin o;
Q_c flow function of vehicle class c;
$\rho_{m,i,c}$ density of vehicle class c in segment (cell) (m,i);
$\rho^{\mathrm{efc}}_{m,i}$ effective density in cell (m,i);
$v_{m,i,c}$ speed of vehicle class c in segment (cell) (m,i);
$v_{\alpha,c}$ speed of vehicle class c in segment (cell) α;
$v^{\mathrm{lim}}_{m,1,c}$ speed that limits the flow for vehicle class c in segment $(m,1)$;
$V_{m,c}$ desired speed function for vehicle class c in link m;
$w_{o,c}$ queue length of vehicle class c at origin o
$d_{o,c}$ external demand of the vehicle class c at origin o;
ρ^{crit}_{m} joint critical density for all vehicle classes in link m;
$\rho^{\mathrm{crit}}_{m,c}$ critical density of vehicle class c in link m;
$\rho^{\mathrm{crit*}}_{m,c}$ parameter of vehicle class c in link m for determining the boundary condition for the semi-congestion regime;
ρ^{max}_{m} effective maximum density in link m;
$\rho^{\mathrm{max}}_{m,c}$ theoretical maximum density of link m if there would be only vehicle class c;
$v^{\mathrm{free}}_{m,c}$ free-flow speed of vehicle class c in link m;
$v^{\mathrm{free}}_{m,\mathrm{max}}$ free-flow speed of the fastest vehicle class in link m;
v^{crit}_{m} joint critical speed for all vehicle classes in link m;
$\delta_{m,c}$ $1+\delta_{m,c}$ is the non-compliance factor of vehicle class c in link m;
$\tau_{m,c}$, $\eta_{m,c}$, $\kappa_{m,c}$, $a_{m,c}$ model parameters of vehicle class c in link m for multi-class METANET;
$C_{o,c}$ theoretical maximum capacity of on-ramp o if there would be only vehicle class c;
w^{max}_{o} maximum allowed queue length for origin o;
$P_{y,c}$ class-dependent parameter matrix for emission (fuel consumption) rates of vehicle class c for emission (fuel) category y;
$\gamma_{1,c}$, $\gamma_{2,c}$ class-dependent model parameters for transferring the fuel consumption rate to the emission rate for CO_2;
$\theta_{m,i,c}$ dynamic passenger car equivalents for vehicle class c in cell (m,i);
$\theta_{o,c}$ dynamic passenger car equivalents for vehicle class c at origin o;
p_c passenger car equivalents for vehicle class c;
$T_{h,c}$ minimum time headway of vehicle class c;
s_c gross stopping distance of vehicle class c;
$\lambda_{m,i,c}$ flow ratio of vehicle class c in cell (m,i);
$\lambda_{o,c}$ flow ratio of vehicle class c at on-ramp o;
Λ_o proportion of the supply that is distributed to on-ramp o;
$D_{m,i,c}$ demand of vehicle class c in cell (m,i);
$D_{o,c}$ total demand of vehicle class c at on-ramp o;
$S_{m,i}$ supply of all vehicle classes in cell (m,i);
$\alpha_{m,i,c}$ road space fraction of vehicle class c in segment (m,i);
$S^{\mathrm{cong}}_{m,i}$ set of all vehicle classes that are in congested mode in segment (m,i);
$S^{\mathrm{free}}_{m,i}$ set of all vehicle classes that are in free-flow mode in segment (m,i);
Y set of emission (fuel) categories;
$a^{\mathrm{inter}}_{m,i,c}$ inter-segment (inter-cell) acceleration of vehicle class c in segment (cell) (m,i);
$a^{\mathrm{cross}}_{\alpha,\beta,c}$ cross-segment (cross-cell) acceleration of vehicle class c from segment (cell) α to segment (cell) β;
$n^{\mathrm{inter}}_{m,i,c}$ number of vehicles corresponding to $a^{\mathrm{inter}}_{m,i,c}$;
$n^{\mathrm{cross}}_{\alpha,\beta,c}$ number of vehicles corresponding to $a^{\mathrm{cross}}_{\alpha,\beta,c}$;
$\mathrm{EM}^{\mathrm{inter}}_{y,m,i,c}$ emission (fuel consumption) rate of emission (fuel) category y corresponding to $a^{\mathrm{inter}}_{m,i,c}$;
$\mathrm{EM}^{\mathrm{cross}}_{y,\alpha,\beta,c}$ emission (fuel consumption) rate of emission (fuel) category y corresponding to $a^{\mathrm{cross}}_{\alpha,\beta,c}$;
$\mathrm{EM}^{\mathrm{inter}}_{\mathrm{fuel},m,i,c}$ fuel consumption rate corresponding to $a^{\mathrm{inter}}_{m,i,c}$;
$\mathrm{EM}^{\mathrm{cross}}_{\mathrm{fuel},\alpha,(m,i),c}$ fuel consumption rate corresponding to $a^{\mathrm{cross}}_{\alpha,(m,i),c}$;
$\mathrm{EM}_{\mathrm{CO}_2,m,i,c}$ emission rate for CO_2 of vehicle class c in segment (cell) (m,i);
$\mathrm{EM}_{\mathrm{fuel},m,i,c}$ fuel consumption rate of vehicle class c in segment (cell) (m,i);
$\mathrm{EM}^{\mathrm{inter}}_{y,o,c}$ emission (fuel consumption) rate of emission (fuel) category y for vehicles in queue at origin o
$u_{0,y,c},\ldots,u_{9,y,c}$ model parameters of vehicle class c for emission category y for multi-class VERSIT+;
$v^{\mathrm{SL}}_{m,i}$ speed limit that is applied in segment (cell) (m,i);
$v^{\mathrm{ctrl}}_{m,i}$ speed limit in segment (cell) (m,i) for a given control step;
r_o ramp metering rate that is applied at on-ramp o;
r^{ctrl}_{o} ramp metering rate of on-ramp o for a given control step;
N_{VSL} number of groups of variable speed limits;
N_{RM} number of groups of metered on-ramps;
J overall objective function;
TTS total time spent;
$\mathrm{TTS}^{\mathrm{end}}$ end-point penalty for total time spent;
$\mathrm{TTS}_{\mathrm{nom}}$ nominal total time spent;
$\mathrm{TTS}^{\mathrm{end}}_{\mathrm{nom}}$ nominal end-point penalty for total time spent;
$t^{\mathrm{rem}}_{m,i,c}$ time that a vehicle of class c that is present in segment (cell) (m,i) at time step $(k_{\mathrm{c}}+N_{\mathrm{p}})M$ would on the average need to get to its destination;
$t^{\mathrm{rem}}_{o,c}$ time that a vehicle of class c present in queue at o at time step $(k_{\mathrm{c}}+N_{\mathrm{p}})M$ would on the average need to get to its destination;
TE_{y} total emissions of emission category y;
$\mathrm{TE}^{\mathrm{end}}_{y}$ end-point penalty for total emissions of category y;
$\mathrm{TE}_{y,\mathrm{nom}}$ nominal total emissions of category y;
$\mathrm{TE}^{\mathrm{end}}_{y,\mathrm{nom}}$ nominal end-point penalty for total emissions of category y;
$\mathrm{TE}^{\mathrm{rem}}_{y,m,i,c}$ emissions that a vehicle of class c present in segment (cell) (m,i) at time step $(k_{\mathrm{c}}+N_{\mathrm{p}})M$ would on the average generate before leaving the network;
$\mathrm{TE}^{\mathrm{rem}}_{y,o,c}$ emissions that a vehicle of class c present in queue at o at time step $(k_{\mathrm{c}}+N_{\mathrm{p}})M$ would on the average generate before leaving the network;
I_{link} set including all the links;
$I^{\mathrm{up}}_{m,i}$ set including all the upstream segments (cells) and origins that connect to segment (cell) (m,i);
I_{all} set of all pairs of link and segment (cell) indices (m,i);
P_{all} set of all pairs of adjacent segments (cells) and origins;
O_{all} set of the indices of all origins;
O_{ramp} set of all metered on-ramps;
I_{speed} set of all segments (cells) with speed limits;
ξ_{TTS}, $\xi_{\mathrm{TE},y}$, ξ_{ramp}, ξ_{speed}, $\xi^{\mathrm{end}}_{\mathrm{TTS}}$, $\xi^{\mathrm{end}}_{\mathrm{TE},y}$ nonnegative weights.

REFERENCES

[1] C. Caligaris, S. Sacone, and S. Siri. Multiclass freeway traffic: Model predictive control and microscopic simulation. In *Proceedings of the 16th Mediterranean Conference on Control and Automation*, pages 1862–1867, Ajaccio, France, June 2008.

[2] K. Aboudolas, M. Papageorgiou, A. Kouvelas, and E. Kosmatopoulos. A rolling-horizon quadratic-programming approach to the signal control problem in large-scale congested urban road networks. *Transportation Research Part C: Emerging Technologies*, 18(5):680–694, October 2010.

[3] S. K. Zegeye, B. De Schutter, J. Hellendoorn, E. A. Breunesse, and A. Hegyi. A predictive traffic controller for sustainable mobility using parameterized control policies. *IEEE Transactions on Intelligent Transportation Systems*, 13(3):1420–1429, September 2012.

[4] M. Hadiuzzaman and T. Z. Qiu. Cell transmission model based variable speed limit control for freeways. *Canadian Journal of Civil Engineering*, 40(1):46–56, January 2013.

[5] G. C. K. Wong and S. C. Wong. A multi-class traffic flow model - an extension of LWR model with heterogeneous drivers. *Transportation Research Part A: Policy and Practice*, 36(9):827–841, November 2002.

[6] M. J. Lighthill and G. B. Whitham. On kinematic waves. II. A theory of traffic flow on long crowded roads. *Proceedings of the Royal Society of London A: Mathematical, Physical and Engineering Sciences*, 229(1178):317–345, May 1955.

[7] P. I. Richards. Shock waves on the highway. *Operations Research*, 4(1):42–51, February 1956.

[8] S. Logghe. *Dynamic Modeling of Heterogeneous Vehicular Traffic*. PhD thesis, K.U.Leuven, Leuven, Belgium, June 2003.

[9] J. W. C. van Lint, S. P. Hoogendoorn, and M. Schreuder. Fastlane: New multiclass first-order traffic flow model. *Transportation Research Record*, 2088:177–187, January 2008.

[10] T. Schreiter, R. L. Landman, J. W. C. van Lint, A. Hegyi, and S. P. Hoogendoorn. Vehicle class-specific route guidance of freeway traffic by model-predictive control. *Transportation Research Record*, 2324:53–62, January 2012.

[11] S. Liu, B. De Schutter, and J. Hellendoorn. Integrated traffic flow and emission control based on FASTLANE and the multi-class vt-macro model. In *Proceedings of the 2014 European Control Conference*, pages 2908–2913, Strasbourg, France, June 2014.

[12] M. Papageorgiou. Some remarks on macroscopic traffic flow modeling. *Transportation Research Part A: Policy and Practice*, 32(5):323–329, September 1998.

[13] A. Hegyi. *Model Predictive Control For Integrating Traffic Control Measures*. PhD thesis, Delft University of Technology, Delft, Netherlands, February 2004.

[14] D. Helbing and A. F. Johansson. On the controversy around Daganzo's requiem for and Aw-Rascle's resurrection of second-order traffic flow models. *The European Physical Journal B*, 69(4):549–562, June 2009.

[15] P. Deo, B. De Schutter, and A. Hegyi. Model predictive control for multi-class traffic flows. In *Proceedings of the 12th IFAC Symposium on Transportation Systems*, pages 25–30, Redondo Beach, California, USA, September 2009.

[16] A. Messmer and M. Papageorgiou. METANET: A macroscopic simulation program for motorway networks. *Traffic Engineering and Control*, 31(9):466–470, September 1990.

[17] A. Kotsialos, M. Papageorgiou, C. Diakaki, Y. Pavlis, and F. Middelham. Traffic flow modeling of large-scale motorway networks using the macroscopic modeling tool METANET. *IEEE Transactions on Intelligent Transportation Systems*, 3(4):282–292, December 2002.

[18] C. Pasquale, I. Papamichail, C. Roncoli, S. Sacone, S. Siri, and M. Papageorgiou. Two-class freeway traffic regulation to reduce congestion and emissions via nonlinear optimal control. *Transportation Research Part C: Emerging Technologies*, 55:85–99, June 2015.

[19] S. Liu, B. De Schutter, and J. Hellendoorn. Model predictive traffic control based on a new multi-class METANET model. In *Proceedings of the 19th World Congress of the International Federation of Automatic Control*, pages 8781–8786, Cape Town, South Africa, August 2014.

[20] T. Zachariadis and Z. Samaras. An integrated modeling system for the estimation of motor vehicle emissions. *Journal of the Air and Waste Management Association*, 49(9):1010–1026, September 1999.

[21] K. Ahn, A. A. Trani, H. Rakha, and M. Van Aerde. Microscopic fuel consumption and emission models. In *Proceedings of the 78th Annual Meeting of the Transportation Research Board*, Washington DC, USA, January 1999. CD-ROM.

[22] N. E. Ligterink, R. De Lange, and E. Schoen. Refined vehicle and driving-behavior dependencies in the VERSIT+ emission model. In *Proceedings of the ETTAP Symposium*, pages 177–186, Toulouse, France, June 2009.

[23] A. Csikós and I. Varga. Real-time modeling and control objective analysis of motorway emissions. *Procedia - Social and Behavioral Sciences*, 54:1027–1036, October 2012.

[24] S. Liu, B. De Schutter, and J. Hellendoorn. Multi-class traffic flow and emission control for freeway networks. In *Proceedings of the 16th International IEEE Conference on Intelligent Transportation Systems*, pages 1334–1339, The Hague, The Netherlands, October 2013.

[25] C. Pasquale, S. Liu, S Siri, S. Sacone, and B. De Schutter. A new emission model including on-ramps for two-class freeway traffic control. In *Proceedings of the 18th IEEE International Conference on Intelligent Transportation Systems*, pages 1143–1149, Las Palmas de Gran Canaria, Spain, September 2015.

[26] R. Courant, K. Friedrichs, and H. Lewy. On the partial difference equations of mathematical physics. *IBM Journal of Research and Development*, 11(2):215–234, March 1967.

[27] A. Hegyi, B. De Schutter, and J. Hellendoorn. Model predictive control for optimal coordination of ramp metering and variable speed limits. *Transportation Research Part C: Emerging Technologies*, 13(3):185–209, June 2005.

[28] C. F. Daganzo. A behavioral theory of multi-lane traffic flow. Part I: Long homogeneous freeway sections. *Transportation Research Part B: Methodological*, 36(2):131–158, February 2002.

[29] G. Pinto and M. T. Oliver-Hoyo. Using the relationship between vehicle fuel consumption and CO_2 emissions to illustrate chemical principles. *Journal of Chemical Education*, 85(2):218–220, February 2008.

[30] E. F. Camacho and C. Bordons. *Model Predictive Control*. Springer-Verlag, London, UK, 2007.

[31] D. Q. Mayne and H. Michalska. Receding horizon control of nonlinear systems. *IEEE Transactions on Automatic Control*, 35(7):814–824, July 1990.

[32] A. Jadbabaie and J. Hauser. On the stability of receding horizon control with a general terminal cost. *IEEE Transactions on Automatic Control*, 50(5):674–678, May 2005.

[33] S. Bera and K. V. Krishna Rao. Estimation of origin-destination matrix from traffic counts: the state of the art. *European Transport\Trasporti Europei*, 49:3–23, December 2011.

[34] K. Parry and M. Hazelton. Estimation of origin-destination matrices from link counts and sporadic routing data. *Transportation Research Part B: Methodological*, 46(1):175–188, January 2012.

[35] E. Cascetta, A. Papola, V. Marzano, F. Simonelli, and I. Vitiello. Quasi-dynamic estimation of o-d flows from traffic counts: Formulation, statistical validation and performance analysis on real data. *Transportation Research Part B: Methodological*, 55:171–187, September 2013.

[36] K. Ahn and H. Rakha. The effects of route choice decisions on vehicle energy consumption and emissions. *Transportation Research Part D: Transport and Environment*, 13(3):151–167, May 2008.

[37] P. M. Pardalos and M. G. C. Resende, editors. *Handbook of Applied Optimization*. Oxford University Press, Oxford, UK, 2002.

[38] L. Davis, editor. *Handbook of Genetic Algorithms*. Van Nostrand Reinhold, New York, USA, 1991.

[39] C. Audet and J. E. Dennis, Jr. Analysis of generalized pattern searches. *SIAM Journal on Optimization*, 13(3):889–903, 2002.

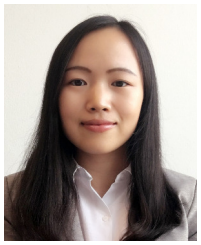

Shuai Liu received the MSc degree in Aeronautical and Astronautical Science and Technology in December, 2011, at National University of Defense Technology in Changsha, China. She is currently a PhD candidate at the Delft Center for Systems and Control of Delft University of Technology in Delft, The Netherlands. Her current research interests are modeling for freeway networks, and robust and distributed control for freeway networks.

Hans Hellendoorn obtained the PhD degree on the topic "Reasoning with Fuzzy Logic" in 1990, at Delft University of Technology, Delft, The Netherlands. Next, he started in 1991 at the Siemens Research Laboratory in Munich in the fuzzy control group. Since 2009 he has been the department head for training simulation at Siemens, The Netherlands. He is currently a full-time professor at the Delft Center for Systems and Control of Delft University of Technology, where he works on traffic management and control.

Bart De Schutter (IEEE member since 2008, senior member since 2010) received the PhD degree in Applied Sciences (summa cum laude with congratulations of the examination jury) in 1996, at K.U.Leuven, Belgium. Currently, he is a full professor at the Delft Center for Systems and Control of Delft University of Technology in Delft, The Netherlands. He is associate editor of the IEEE Transactions on Intelligent Transportation Systems. His current research interests include control of discrete-event and hybrid systems, multi-level and distributed control, and intelligent transportation and infrastructure systems.